An implantable bi-directional wireless transmission system for transcutaneous biological signal recording

Chih-Kuo Liang[1]**, Jia-Jin Jason Chen**[2]**, Cho-Liang Chung**[3]**, Chen-Li Cheng**[4] **and Chua-Chin Wang**[5]

[1] Department of Electrical Engineering, Southern Taiwan University of Technology, Tainan County, Taiwan, Republic of China
[2] Institute of Biomedical Engineering, National Cheng Kung University, Tainan, Taiwan, Republic of China
[3] Department of Materials Science and Engineering, I-Shou University, Kaohsiung County, Taiwan, Republic of China
[4] Division of Urology, Department of Surgery, Taichung Veterans General Hospital, Taichung, Taiwan, Republic of China
[5] Department of Electrical Engineering, National Sun Yat-sen University, Kaohsiung, Taiwan, Republic of China

E-mail: jason@jason.bme.ncku.edu.tw

Abstract

This study presents an implantable microcontroller-based bi-directional transmission system with an inductive link designed for biological signal sensing. The system comprises an external module and an implantable module. The external module incorporates a high-efficiency class-E transceiver with amplitude modulation scheme and a data recovery reader. The transceiver sends both power and commands to the implanted module, while the reader recovers the recorded biological signal data and transmits the data to a personal computer (PC) for further data processing. To reduce the effects of interference induced by the 2 MHz carrier signal, the implanted module uses two separate coils to perform the necessary two-way data transmission. The outward backward telemetry circuitry of the implanted module was based on the load-shift keying (LSK) technique. The transmitted sensed signal had a 10-bit resolution and a read-out rate of 115 kbps. The implanted module, measuring $4.5 \times 3 \times 1.2$ cm^3, was successfully verified in animal experiment in which the electroneurogram (ENG) signal was recorded from the sciatic nerve of New Zealand rabbits in response to nociceptive stimulation of foot. The reliable operating distance of the system was within about 3.5 cm with an efficiency of around 25%. Our present study confirms that the proposed biological signal sensing device is suitable for various implanted applications following an appropriate biocompatible packaging procedure.

(Some figures in this article are in colour only in the electronic version)

1. Introduction

Physiologists and scientists have been seeking to develop wireless and implantable sensing devices for direct and reliable measurement of biological signals which are difficult to access using surface recording techniques (Mackay 1993, Nagel 1984). However, the low transmission rates of typical commercial telemeters limit their application to the recording of biological signals where a low sampling rate is sufficient, e.g. electrocardiograms (ECG), blood pressure, intracranial pressure, body temperature, etc. (Hansen *et al* 1982, Chatzandroulis *et al* 2000, Manwaring *et al* 2001, Schierok *et al* 2000). Although analog transmission protocols via frequency modulation technique could eliminate the requirement for a sampling process, they are susceptible to noise and support a restricted number of recording channels. Hence, these protocols tend to be unsuitable for neural signal recording applications. Alternative approaches which extract the features of the biological signal, e.g. the firing intervals from the neural signal, rather than transmitting the raw signal in its entirety (Akin *et al* 1998, Donaldson *et al* 2003) are impractical in certain regards. Recent research increasingly requires the raw signal, and particularly the high-frequency neural signal, to be recorded and acquired while the animal is conscious and with minimal constraint (Yu and Najafi 2001).

Implementing wireless transmission for passive implanted devices involves two key design issues, namely the transcutaneous coupling of the power and commands to the implanted module and the subsequent outward transmission of the sensed data. Regarding the inward transmission, the efficiency of the power coupling and the demodulation of the inward data are two major concerns. In a transcutaneous coupling, the commands are embedded in a radio frequency (RF) carrier signal, which also transmits the necessary power to drive the battery-free implant (Huang and Oberle 1998, Murakawa *et al* 1999). An inductive link between the external and internal modules is generally preferred since this particular arrangement yields a high-power coupling efficiency and is typically less complex. The inductive link is particularly suitable for powered implants within an acceptable close distance (Heetderks 1988, Troyk and Schwan 1992, Akin *et al* 1998).

Two coupling strategies are commonly employed to facilitate the backward telemetry of data from the implant to the external module. One approach is simply to use the same inductive field as the inward transmission medium and to utilize the impedance reflection principle to convey the data (Tang *et al* 1995). The second approach is to use an additional RF carrier field as the transmission medium and to employ an appropriate modulation technique (Donaldson *et al* 2003, Puers *et al* 2000, Ghovanloo and Najafi 2003). For the case of bi-directional power and data transmission, the former approach is less complicated than the latter. Typically, bioelectrical measurements involve low-intensity signal sources in the μV to low mV range. However, the magnetic coupling signal of the inductive coupling may be several orders of magnitude larger than these recorded biological signals (Gudnason *et al* 2001). The high intensity of the magnetic flux may introduce undesirable interference during the outward telemetry of the data and may even cause the microcontroller of the internal module to fail. Therefore, when designing the outward transmission scheme, a compromise must be achieved
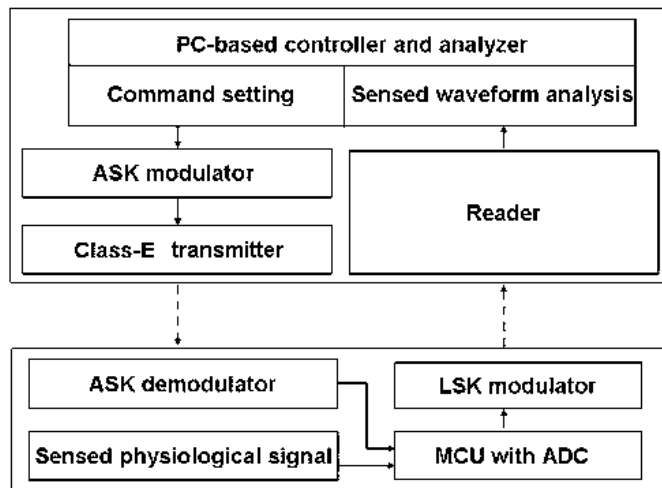
Figure 1. Flowchart of simultaneous inward transmission of power and commands as well as subsequent outward transmission of recorded biological signals.

among noise immunity, power consumption, physical size, effective transmission distances and attainable transmission rates. These design issues are particularly important when measuring low-sensitivity biological signals such as the electroneurogram (ENG) signals considered in the current study.

The objective of the present study was to implement a bi-directional wireless system for a battery-free implantable sensing device. The validity of the proposed design was confirmed by applying the developed biomicrosystem to the sensing and transmission of ENG signals acquired from rabbit's sciatic nerve via a cuff electrode. The functional blocks of the proposed wireless system were verified through animal studies. These results demonstrate the potential applications of the system for varied implanted biological measurements.

2. Materials and methods

Figure 1 presents a flowchart of the inward transmission of power and commands to the implanted module and the subsequent outward transmission of the sensed data. A PC-based controller utilizes a graphic user interface (GUI) developed by using LabVIEW software to specify the sensing configuration required for data acquisition as well as to visualize the data. The current wireless transmission setup adopts the half-duplex transmission mode in which either the inward commands or outward sensed data were transmitted wirelessly. Initially, the internal module is in an idle condition, waiting to receive commands from the external controller. The command data, 8-bit in length, include the resolution specification, the ADC channel specification and the sampling rate specification. Having sensed the signal data, the internal module transmits the sensed data to the external module via inductive coupling. During the data outward transmission period, the external transceiver simply transmits a pure power carrier signal to the internal module which can minimize the interference.

Two physical parts, namely the internal implantable sensing module and the external control module, as well as their layout for transcutaneous recording of ENG from a partially constraint rabbit are depicted in figure 2. The details of each block and experimental procedure are described in the following sections.
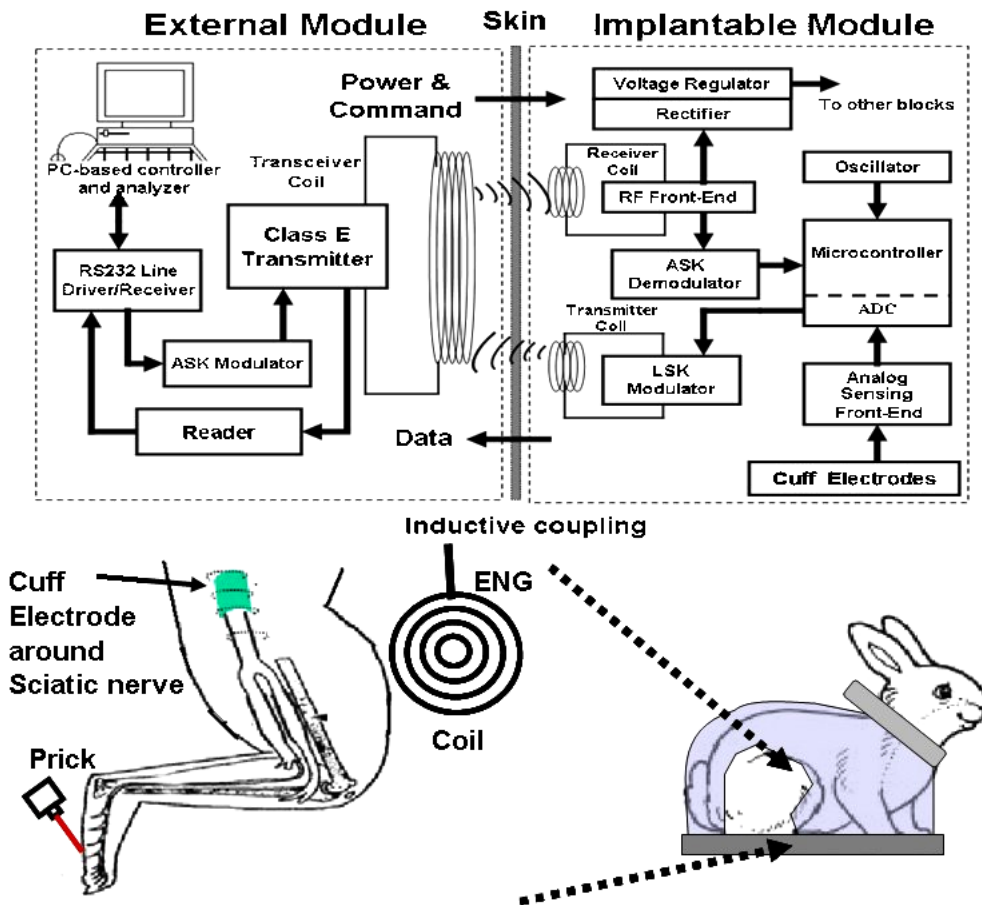
Figure 2. Block diagram of implantable sensing system including the external module with class-E power amplifier and reader as well as internal module with data/power recovering circuit, analog sensing front end and LSK modulator for outward transmission. The implanted module is validated in transcutaneous coupling of ENG from a rabbit when it is awake but partly constrained in a rabbit restrainer.

2.1. Inward transmission of power and commands

Several researchers have successfully demonstrated the use of amplitude-shift keying (ASK) modulation and high-efficiency class-E power amplifiers for inward transmission of power and commands simultaneously (Heetderks 1988, Troyk and Schwan 1992, Zierhofer and Hochmair 1990, Ziaie *et al* 2001). The class-E amplifier scheme is adopted in this study and modified with more stable feedback loop.

2.1.1. Class-E RF transceiver. As shown in the upper part of figure 3, the general class-E power amplifier includes a series resonant tank (i.e. L_{tr} and C_{s1} in series with C_{s2}), a parallel resonant tank (i.e. L_{tr} and C_p), a series-connected choke (L_{choke}) and a high-speed N-type power MOSFET, which drives the resonant network. Besides the class-E amplifier, the transceiver also includes two other basic components, namely a feedback control circuit and an ASK modulation circuit (Liang *et al* 2003).
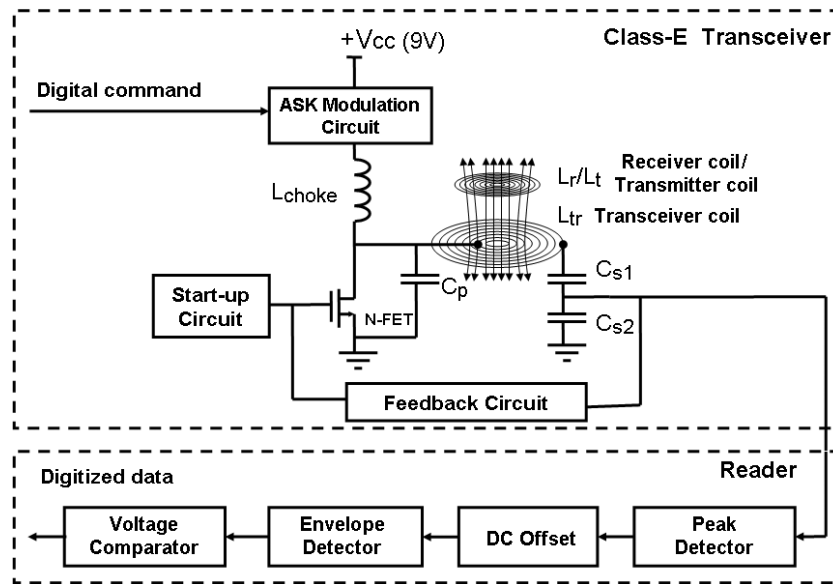
Figure 3. Schematic representation of external module comprises the class-E transceiver and the reader.

Previous studies have shown that the use of a closed-loop feedback stabilizes the class-E operation mode in the event of variations in the transceiver coil inductance and indirectly improves the amplifier's efficiency (Troyk and Schwan 1992, Zierhofer and Hochmair 1990). Our modified feedback control circuit comprises a two-cascaded CMOS inverter connected to a RC phase tuner. The choke inhibits impulses from the drain terminal of the driving MOSFET and provides the means to pass a steady dc current. The voltage in the current resonant network is rather high and cannot pass through the feedback circuit directly. Hence, C_{s1} and C_{s2} are used as series capacitive voltage dividers to generate a smaller voltage for feedback circuit. In the resonant state, the high peak resonant current of the series branch, including the transceiver coil, L_{tr} and the capacitors (C_{s1} and C_{s2}), may increase the power loss due to the thermal effects of being non-ideal components. Therefore, the current setup specifies negative/positive zero-temperature-coefficient (NPO) capacitors as the capacitive components and employs high-Q Litz wire for the transceiver coil. This approach alleviates the shift in resonant frequency caused by the Ohmic loss, I^2R.

This study deliberately adopts the ASK modulation approach in preference to frequency or phase modulation techniques in an attempt to achieve a balance between the system performance and the component requirements (Marschner *et al* 2003, Zierhofer and Hochmair 1990). The current ASK modulation circuit comprises a Darlington pair of transistors and two series voltage-divided resistors connected via a MOSFET switch to modulate the 2 MHz carrier signal (Ziaie *et al* 2001). The selection of modulation frequency must consider the attenuation of magnetic field intensity in air (non-magnetic material) and the power absorption of biological tissue with the eddy current induced by a magnetic field. A low carrier frequency could cause a too slow and undesirable data transmission rate. However, a higher carrier frequency will produce extra heat, which might cause injury to the body tissue. These possible power dissipations leading to thermal effects in body tissues should be noted and controlled for satisfying safety guidelines (Litvak *et al* 2002). Our selection of 2 MHz carrier frequency is within the range, hundreds of kHz to 20 MHz, suggested by researchers for implantable microstimulator or biomicrosystem (Ziaie *et al* 1997, Smith *et al* 1998).

The digital command input from the PC-based controller acts as a pulse trigger which alternately switches this MOSFET switch on and off, thereby forming a two-level dc supply. The optimally selected choke (Sokal 2000) in the class-E amplifier tends to suppress rapid signal changes and therefore slows the modulation rate. However, the volume of the command data is relatively small in the current case, and hence the slower transmission rate does not cause a significant deterioration of the system performance.

2.1.2. Internal power and command recovery unit.   The battery-free implanted module is powered by the external power transmitter via an RF link. The distance separating the two sets of coupling coils and the match in the coil sizes need to be carefully considered, otherwise the implant could receive very little power. Generally, the magnetic flux density in air outside the primary coil drops steeply for distances greater than its average radius, thus the coupling coefficient is very low, typically <3% (Loeb *et al* 2001, Ziaie *et al* 1997, Zierhofer and Hochmair 1990). Therefore, designing a high-Q circuitry is absolutely necessary for getting enough power within a reasonable distance.

The overall power and data recovery circuitry, which includes a receiving LC resonant tank, a power regulator, including rectifier and voltage stabilizer, and three-staged ASK demodulator, are depicted in the right column of figure 2. When the class-E power amplifier transmits the power and embedded commands via the electromagnetic coupling, the LC parallel resonant tank is tuned such that its resonant frequency corresponds to the 2 MHz carrier frequency of the external transmitter. The power supply of the implant is stabilized to ± 3 V by means of zener diodes and a negative voltage converter (ICL7660). The negative supply voltage then drives the analog sensing front-end as it performs physiological signal measurement.

To recover the digital commands, the ASK data demodulator recovers the original command data from the modulated RF wave. This is a three-staged process and is composed of an envelope detector, a voltage divider and an inverter after the same LC resonant tank of power recovery. The envelope detector, which consists of a low-pass filter and a high-pass filter, extracts the high–low signal variation of the 2 MHz carrier wave with a dc offset. The values of resistor and capacitor at the output of the envelope detector should be carefully chosen so as to optimize the demodulation process (Zierhofer and Hochmair 1990). The voltage divider is used to reduce the detected digital commands to a required level after the inverter for microcontroller operation.

2.2. Outward transmission of sensed data

Having received the combined power and command signal, the internal module sets up the sampling rate and channel for sensing the biological signals and then executes backward telemetry with the external module to transmit the sensed data to a PC for further processing. In the present study, the implantable module is constructed entirely of surface mount device (SMD) type components and includes two separate inductive coils. The internal module is mounted on a double-layered PCB measuring $4.5 \times 3 \times 1.2$ cm^3. The receiver coil is 2.5 cm in diameter and the transmitter coil is wound around the perimeter of the printed circuit board. The photograph of the implantable sensing device before casting with its receiver and transmitter coils, and of the developed RF transceiver coil, is shown in figure 4. The key components of the outward transmission path are presented in the following sections.

2.2.1.   Sensing front-end and microcontroller unit for data acquisition.   Low-noise instrumentation amplifiers with high common mode rejected ratios (CMRR) (>110 dB at
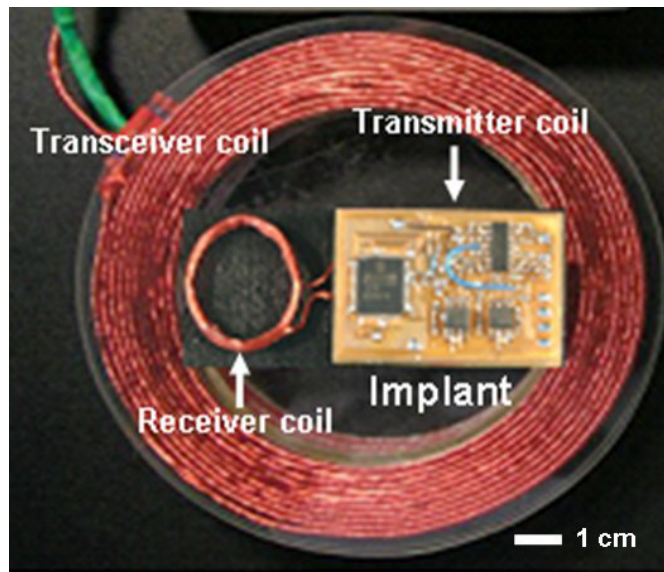
Figure 4. Photograph of the implantable wireless sensing module before casting with receiver coil (for inward power/command receiving) and transmitter coil (for outward data transmission), and of the transceiver coil of external reader.

gain = 1000) (IA, INA118) are used to perform an initial amplification of the recorded biological signals. A quasi-tripolar cuff electrode is used to sense the ENG signals from the peripheral nerve (Donaldson *et al* 2003). The recorded signals are amplified (gain: 10 000) and band-pass filtered and are then digitized by an analog-to-digital converter (ADC) at 10-bit resolution. The data acquisition process is controlled by an SMD-type microcontroller (PIC18F452) with embedded ADCs. The entire sensing front-end is shielded to minimize the effects of magnetic interference.

2.2.2. Load-shift keying (LSK) unit for outward coupling. The current implantable device uses a two-coil strategy to protect the weak biological signals from the effects of the strong RF electromagnetic fields generated by the inductive coupling. The impedance reflection technique, utilizing a LSK modulation method, is generally adopted in implantable biomicrosystem applications (Smith *et al* 1998, Gudnason *et al* 2001, Lanmüller *et al* 1999). This study adopts the LSK unit, shown in figure 5, which is modified from the unit described previously by Tang *et al* (1995). The modified LSK scheme exploits the fact that a variation in the pre-designed load impedance of the internal circuitry is reflected to the transceiver coil by an inductive link. It is noted that the current approach uses only one pair of series resistors (R_1 and R_2) in parallel with the LC resonant tank (C_t and L_t), operating at a 2 MHz carrier frequency as described previously. The series resistors are connected to a MOSFET switch, which permits the generation of two different reflected impedances. Consequently, high–low voltages are induced in the primary resonant loop of the class-E transceiver.

2.2.3. External reader for recovering sensed signal. The function of the external ASK demodulation circuit is to extract the very small high–low fluctuating signal generated by the LSK modulation of the carrier waveform via the voltage divider (formed by C_{s1} and C_{s2}) in
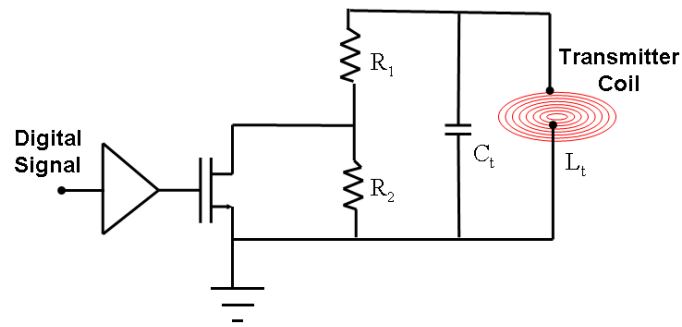
Figure 5. The outward transmission of sensed digital data is modulated in LSK scheme by switching between two resistance loads, R1 + R2 and R1 to the LC resonant tank.

the series resonant tank of the class-E amplifier. As shown in the lower part of figure 3, the reader (i.e. the LSK demodulator) consists of a peak detector, an adjusting circuit for the dc offset, an envelope detector and a voltage comparator. The ASK signal received from the LSK modulator has a very weak signal-to-noise ratio, typically around 1:150 in our cases. The peak detector serves only to detect the modulated signal. The envelope detector extracts the LSK modulated signal from the 2 MHz carrier signal. The demodulated signal with a dc offset is then passed through the voltage comparator for level adjustment and transmitted to the PC via an RS-232 interface.

2.3. Validation of implanted sensing device

Before implantation, biocompatible packaging of the designed wireless sensing device is desirable. The polymer, silicon rubber was selected as a candidate for the packaging material due to its biocompatibility and easy process. The dam-and-fill packaging technique was applied to encapsulate the internal circuit. The dam-and-fill is a two-step encapsulation process including the dispensing of higher-viscosity encapsulant around the component to form a dam and the fill of dam with a lower-viscosity material. After dam-and-fill encapsulation, the implantable device was coated with a layer of biocompatible material, silicon rubber (Nusil[TM] 1137), which was accomplished within a custom-made Teflon mold. The implantable sensing module was measured regularly through a sinusoidal signal connected to the input of sensing front-end when it was placed in normal saline solution for *in vitro* hermeticity test. Similar encapsulation process can be found in our previous approach for an implantable microstimulator (Hung *et al* 2003).

   After *in vitro* evaluation, the developed wireless sensing module was employed to record and transmit the whole nerve electrical activity of ENG from conscious rabbit. Six male white rabbits of New Zealand weighting 2–3 kg were anesthetized with ketamine hydrochloride via an intravenous injection (3 mg kg^{-1} min^{-1}, i.v.). A self-coiling spiral tripolar-nerve cuff electrode, of length 20 mm and distance 6 mm between the rings, was mounted on the right sciatic nerve, and a hermetically sealed internal module implanted within subcutaneous tissue over the lateral side of the hindleg. All implanted devices were first rinsed with 95% ethanol and then with deionized water before being sterilized by UV light (245 nm) for 30 min and dried overnight. After surgery, an antibiotic cream was applied to the wound to prevent inflammation and the animal returned to its cage. Experiments began after 7 days post-operative recovery. All of the experimental procedures used in this study complied with National Cheng Kung University Hospital Regulations for animal use and care.

For the sake of simplicity, a mechanical stimulation approach was adopted to activate the nociceptive pathway. The awake rabbits were restrained in a standard restraining device, in which animals cannot move and which leads to their relaxation. There was therefore no spontaneous activity in the motor axons of the nerve during the recordings. Specifically, a sharp plastic tip mounted on an electric solenoid actuator was used to prick the sole of the rabbit's right foot, which can be programmed at a desired frequency and force to achieve the level of mechanical stimulation necessary to activate the receptors. The force applied was set in the range to activate mechanoreceptors and induce nerve activity without eliciting a visible withdrawal reflex. The external sensing coil was placed close to the right hind limb for acquiring the ENG resulting from the nociceptive sensing. A software control program is used to synchronize the wireless transmitted ENG and the recording of prick duration.

3. Results and discussion

3.1. Inward transmission of power and commands

In designing a mechanism for the simultaneous inward transmission of power and data commands, the selection of a round receiver coil for both the external transceiver and the internal transmitter coils simplifies the computation and design of the coupling inductance. This approach not only increases the efficiency of the inductive coupling, but also renders the inductively coupled coil system insensitive to misalignment of the various coils (Troyk and Schwan 1992). The transceiver coil was made of Litz wire (strands 48 AWG) formed of multi-twisted thin lines with 8 bundles in a line and 175 strands in a bundle. It has an outer diameter of 9 cm and an inner diameter of 7 cm. A high Q value ($Q = 470$) and a high inductance value (21 μH with 13 turns) can be obtained, compared to the same cross-sectional area made from general solid wire. Therefore, the class-E transmitter could consume less power and provide a superior coupling efficiency. However, it is noted that an excessive Q value can lead to an over sensitivity of the coupled RF signal to any lateral or longitudinal displacements between the transceiver and receiver coils.

The receiver coil (8.6 μH inductance) of the developed implanted module has the ability to couple RF signals between 10 V and 30 V when the distance between the transceiver and receiver coils falls within an effective range. The front end of the RF receiver in the implanted unit incorporates two regulators which rectify the voltage into +3 V for the digital circuit and ±3 V for the analog circuit, respectively. Our previous results indicated that the outputs of the regulated voltages fluctuate within a narrow range of approximately 0.2 V within a 35 mm coupling distance (Peng *et al* 2004). Within this coupling distance, it is found that the demodulated output digital signal can always be maintained at the desired logical levels (0 V and 3 V).

Figure 6(a) shows the amplitude modulated RF 2 MHz carrier signal carrying both power and data commands. It is noted that this signal is measured at the terminal of the internal power/command coil. Figure 6(b) presents the corresponding recovered data commands obtained from the ASK data demodulator in the implanted module. It can be seen that most of the RF waveform is associated only with power transmission. However, some part of the waveform is used for the transmission of both power and data commands when necessary, e.g. when the sampling rate and the channel are to be sent to the implanted module. When the external module is activated, a continuous RF power is transmitted to power the implant. During data command transmission, the digital data observed being a continuous power carrier with about 5% modulation index are transmitted to the implant. The current study specifies a relatively low modulation ratio, which satisfies the power demands of the implant
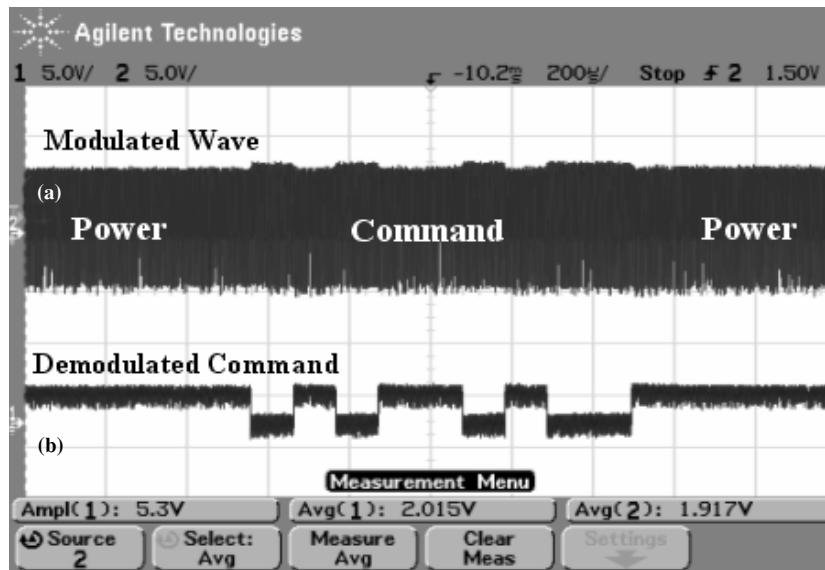
Figure 6. (a) The 2 MHz carrier signal by ASK modulation measured at terminal of receiver coil in ASK demodulator unit, and (b) the corresponding demodulated digital command signal.

by compromising on the transmission rate of the modulated signals. However, as discussed previously, the data length of the commands transmitted to the implanted module is relatively low in the current case and hence high transmission rates are unnecessary. An optimal system performance can therefore be achieved via a careful tuning of the demodulation circuit in the receiver circuit.

During inward command transmission, the digital commands are integrated and arranged into an 8-bit predefined data format. After coding from the PC-based analyzer, the serial data stream is sent to the class-E transmitter with a maximum data transmission rate of 57.6 kbps.

3.2. Outward transmission of data

Figure 7 exhibits the sequences of outward transmission of digital signals. The clear digital signal (figure 7(a)) is the output of the ADC terminal of the PIC18F452 microcontroller which causes a small fluctuation in the modulated RF carrier with peak-to-peak voltage around 150 V measured in LSK terminal of external reader after outward digital transmission (figure 7(b)). From its expanded view in figure 7(d), the digital signal voltage fluctuation on the RF carrier is comparatively small and is usually less than 1 V. In addition, the observed impulse noises are induced by the switching effect of the inductor in the transformer-type link and possibly also by the delay effect caused by self-oscillation of the class-E feedback loop, which is difficult to inhibit entirely.

Although the sensing signal voltage fluctuation is very small, the designed ASK demodulator (i.e. the reader) is nevertheless capable of performing an effective decoding of the digitized data contained in the carrier wave. The recovered digital signal and the signal after level adjustment before input to the serial port of PC are shown in figures 7(e) and (f), respectively. These results confirm that the current outward transmission and demodulation arrangement permits the sensed data to be recovered cleanly. The following example of ENG sensing verifies this function.
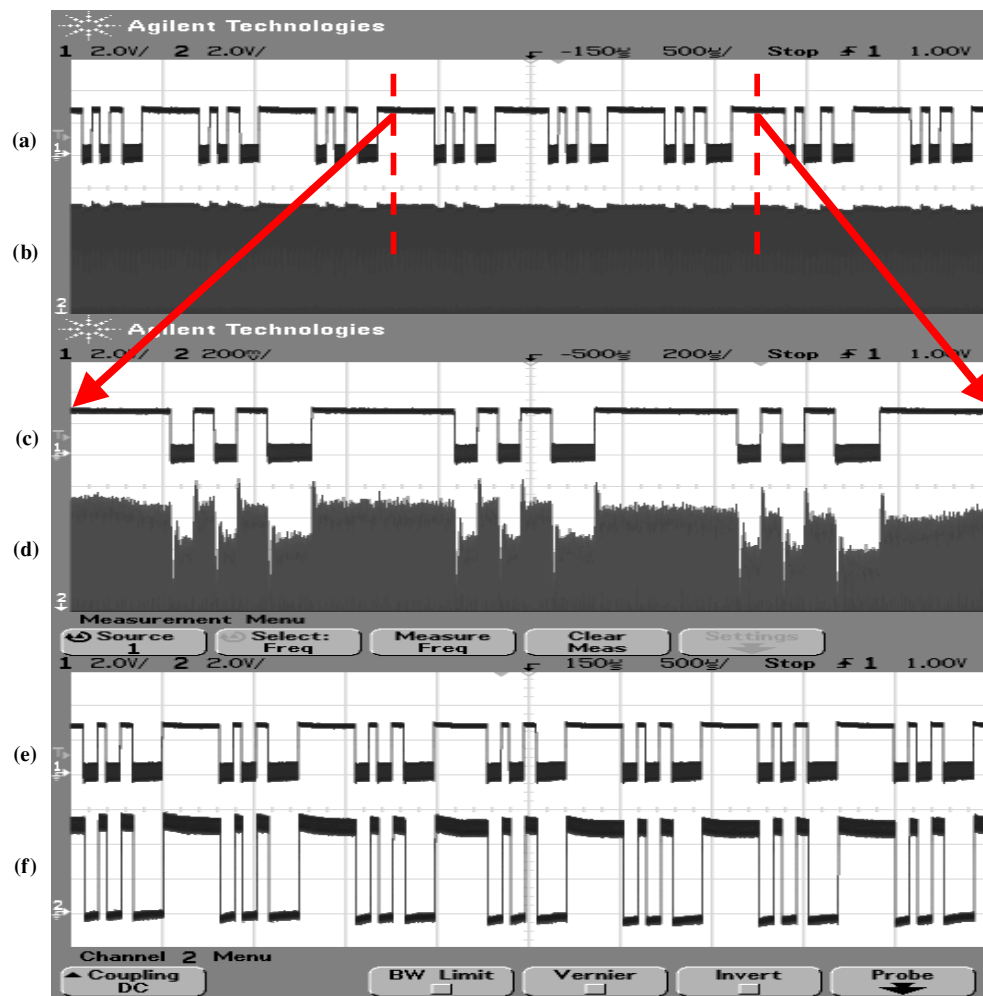
Figure 7. The sensed digital data (0–3 V) (a) cause a small fluctuation in the LSK modulated carrier signal of 2 MHz at around 150 V (partly shown in b). Corresponding to the digital data in (c), small digital signal (<1 V) and pulse-like noises can be seen in the carrier from the enlarged view in (d). The digital signals after peak detector and envelope detector (e) and level adjustment (f) are ready for sending to PC.

3.3. Validation and system performance

Before *in vivo* implantation, *in vitro* tests were performed by placing implantable module in normal saline solution and recorded sinusoidal signal once a day. The long-lasting wireless sensing device survived for a period of 30 days for *in vitro* test. This implies that the sealing of current implantable sensing module is feasible for short-term animal trial but not for a chronic implantation greater than one month.

Figure 8 presents a representative nociceptic signal sensed from a rabbit's sciatic nerve as acquired using the proposed wireless sensing device. The pulses indicate instances of pricking the sole of the rabbit's foot for 1 s duration. The induced ENG responses are clearly observed. The original background signal level is approximately ±6 μV, but following pricking of the sole, the amplitude of the ENG signal increases rapidly to a value of approximately ±20 μV.
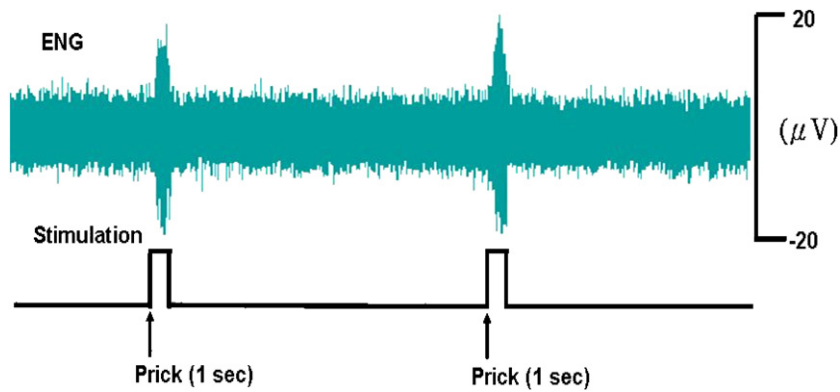
Figure 8. Nociceptic signals acquired from rabbit's sciatic nerve via implanted sensing module with miniature cuff electrode.
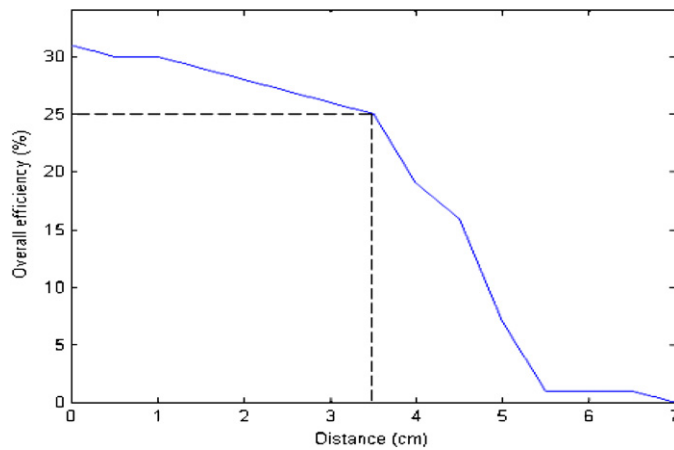
Figure 9. Overall system efficiency along the coupling distance between external transceiver coil and implanted receiver coil.

The average signal-to-noise ratio (average power of signal/average power of noise) of the ENG measurements of our six successful implantation of rabbits is 10.5 ± 1.2. The present set-up permits a maximum sampling rate of 11 kHz, which is sufficient to cope with electrophysiological recordings of signals containing frequencies up to around 5 kHz, including the commonly employed EMG, EEG and ENG recordings.

The overall power dissipation of the implanted system is just 90 mW (approximately). This low power consumption is an essential design criterion, particularly for implanted devices with no internal battery, as in the current case. Figure 9 shows the overall system efficiency as a function of the coupling distance in air. The efficiencies of the power amplifier and the RF electromagnetic coupling play particularly significant roles in determining the power loss incurred during wireless transmission. With an appropriate tuning of the switching point, the self-oscillating class-E power amplifier can provide very high power transmission efficiency, typically greater than 90%. However, the present results reveal that the power coupling efficiency decreases significantly as the coupling distance increases, such that by 55 mm, it has fallen to 1%. The maximum permissible coupling distance between the internal and external modules was found to be around 35 mm, where the overall efficiency reaches 25%.

This limit to the coupling distance can be attributed to the low coupling coefficient arising from the use of a small receiver coil and the poor magnetic conduction properties of air. Although the current coupling efficiency can be increased by equipping the implanted receiving coil with a miniature ferrite core, this approach would inevitably increase the size of the implanted module. Although the transmission distance between the two modules can be extended by increasing the size of the external transceiver coil, an intense RF electromagnetic wave may actually be counterproductive since it may affect the electronic circuits of the internal module and/or the control sequence of the implanted microcontroller.

4. Conclusions

We have implemented a wireless bi-directional implanted sensing device by using discrete electronic components. This prototype of implantable sensing device is built on a double layered rectangular PCB in $4.5 \times 3 \times 1.2$ cm^3, where overall power consumption of implanted device was measured around 90 mW. The maximum reliable operating distance between the transceiver coil and receiver coil reaches about 3.5 cm under the overall efficiency of 25%. A low-power, high-performance circuit block has been adopted and modified that is crucial for implantable device utilizing wireless RF telemetry for power and data transmission by ASK modulation. However, the interference of strong electromagnetic wave could saturate the preamplifier and cause interference in the sensed weak biological signal. Therefore, two pairs of coupling coils were implemented in the implantable module in an attempt to alleviate the magnetic interference induced by the inductive coupling. The LSK strategy and its corresponding demodulator (reader) were developed for back telemetry, and that obtained good results from ENG validation tests.

All the functions of the prototype implantable sensing device have been verified successfully so that it could be used for other physiological recordings of animals and for a basis of developing miniature device using application-specific integrated circuit design (Salmons *et al* 2001) in the next stage. Incorporated with properly selected sensors, the implantable device can be applied to various biological signal measurements. Although our implantable sensing device has been evaluated in both *in vitro* and *in vivo* tests for up to 30 days, the hermetic package of implanted device for long-term chronic implantation should be further investigated to ensure that the body fluid would not induce malfunctions of the device. Our ongoing project is to integrate this implantable sensing device with programmable microstimulation module for varied physiological studies. For example, a combined sensing/stimulation module can be used for investigating the long-term effect of implanted cuff electrode by *in vivo* measuring the impedance between electrodes and peripheral nerve.

Acknowledgments

References

Akin T, Najafi K and Bradley R M 1998 A wireless implantable multichannel digital neural recording system for a micromachined sieve electrode *IEEE Trans. Solid-State Circuits* **33** 109–18

Bradley R M, Cao X, Akin T and Najafi K 1997 Long term chronic recording from peripheral sensory fibers using a sieve electrode array *J. Neurosci. Methods* **73** 177–86

Chatzandroulis S, Tsoukalas D and Neukomm P A 2000 A miniature pressure system with a capacitive sensor and a passive telemetry link for use in implantable applications *J. Microelectron. Syst.* **9** 18–23

Donaldson N de N, Zhou L, Perkins T A, Munih M, Haugland M and Sinkjaer T 2003 Implantable telemeter for long-term electroneurographic recordings in animals and humans *Med. Biol. Eng. Comput.* **41** 654–64

Ghovanloo M and Najafi K 2003 A fully digital frequency shift keying demodulator chip for wireless biological implants *IEEE-SSMSD* 223–7

Gudnason G, Nielsen J H, Bruun E and Haugland M 2001 A distributed transducer system for functional electrical stimulation *IEEE Electronics, Circuits and Systems 8th Int. Conf.* **1** 397–400

Hansen B, Aabo K and Bojsen J 1982 An implantable external powered radio-telemetric system for long term ECG and heart-rate monitoring *Biotelem. Patient Monit.* **9** 227–37

Heetderks W J 1988 RF powering of millimeter and submillimeter sized neural prosthetic implants *IEEE Trans. Biomed. Eng.* **35** 323–7

Huang Q and Oberle M 1998 A 0.5-mW passive telemetry IC for biomedical applications *IEEE Trans. Solid-State Circuits* **33** 937–46

Hung C C, Chung C L, Lin K P, Young G S and Chen J J J 2003 Packaging design for implantable microstimulator *J. Med. Biol. Eng.* **23** 129–36

Kazimierczuk M K and Czarkowski D 1995 *Resonant Power Converters* (New York: Wiley) pp 347–78

Lanmüller H, Sauermann S, Unger E, Schnetz G, Mayr W, Bijak M, Rafolt D and Girsch W 1999 Battery-powered implantable nerve stimulator for chronic activation of two skeletal muscles using multichannel techniques *Artif. Organs* **23** 399–402

Liang C K, Yang G S, Chen J J J and Chen C K 2003 A microcontroller-based implantable stimulation system with wireless power data transmission for animal neuromuscular experiments *J. Chin. Inst. Eng.* **26** 493–501

Litvak E, Foster K R and Repacholi M H 2002 Health and safety implications exposure to electromagnetic fields in the frequency range of 300 Hz to 10 MHz *Bioelectromagn.* **23** 68–82

Loeb G E, Peck R A, Moore W H and Hood K 2001 BION™ system for distributed neural prosthetic interfaces *Med. Eng. Phys.* **23** 9–18

Mackay R S 1993 *Bio-Medical Telemetry: Sensing And Transmitting Biological Information From Animals And Man* (New York: IEEE Press)

Manwaring M L, Malbasa V D and Manwaring K L 2001 Remote monitoring of intracranial pressure *Ann. Acad. Studenica* **4** 77–80

Marschner C, Rehfuss S, Peters D, Bolte H and Laur R 2003 A novel circuit concept for PSK-demodulation in passive telemetric systems *Microelectron. J.* **33** 69–75

Murakawa K, Kabayashi M, Nakamura O and Kawata S 1999 A wireless near-infrared energy system for medical implants *IEEE Eng. Med. Biol.* Nov/Dec 70–2

Nagel J H 1984 Passive biotelemetry systems *Biomed. Eng.* **31** 577–9

Peng C W, Chen J J J, Poon W F, Lin C C and Lin K P 2004 Effects of selective stimulation and blocking on nerve fibers via an implantable microstimulator system. *J. Neurosci. Method* **134** 81–90

Puers R, Catrysse M, Vandevoorde G, Collier R J, Louridas E, Burny F, Donkerwolcke M and Moulart F 2000 A telemetry system for the detection of hip prosthesis loosening by vibration analysis *Sensors Actuators* **85** 42–7

Salmons S, Gunning G T, Taylor I, Grainger S R W, Hitchings D J, Blackhurst J and Jarvis J C 2001 ASIC or PIC implantable stimulators based on semi-custom CMOS technology or low-power microcontroller architecture *Med. Eng. Phys.* **23** 37–43

Schierok H, Markert M, Pairet M and Guth B 2000 Continuous assessment of multiple vital physiological functions in conscious freely moving rats using telemetry and a plethysmography system *J. Pharm. Toxicol. Methods* **43** 211–7

Sinkjaer T, Haugland M, Strujik J and Riso R 1999 Long-term Cuff electrode recordings from peripheral nerves in animals and humans *Modern Techniques in Neuroscience* ed U Windhorst and H Johansson (New York: Springer) pp 787–802

Smith B, Tang Z, Johnson M, Pourmehdi S, Gazdik M, Buckett J and Peckham P 1998 An externally powered, multichannel, implantable stimulator-telemeter for control of paralyzed muscle *IEEE Trans. Rehabil. Eng.* **45** 463–75

Sokal N O 2000 Class-E switching-mode high-efficiency tuned RF/microwave power amplifier: improved design equations *IEEE Microw. Theory Techn. Soc. Dig.* **2** 779–82

Tang Z, Smith B, Schild J H and Peckham P H 1995 Data transmission from an implantable biotelemeter by load-shift keying using circuit configuration modulator *IEEE Trans. Biomed. Eng.* **42** 524–8

Towe B C 1986 Passive biotelemetry by frequency keying *IEEE Trans. Biomed. Eng.* **33** 905–9

Troyk P R and Schwan M A K 1992 Closed-loop class E transcutaneous power and data link for micro-implants *IEEE Trans. Biomed. Eng.* **39** 589–99

Yu H and Najafi K 2001 Circuitry for a wireless microsystem for neural recording microprobes *Proc. 23rd Annual Int. Conf. of the IEEE Engineering in Medicine and Biology Society* vol 4132, pp 761–4

Ziaie B, Nardin M D, Coghlan A R and Najafi K 1997 A single-channel implantable microstimulator for functional neuromuscular stimulation *IEEE Trans. Biomed. Eng.* **44** 909–20

Ziaie B, Rose S C, Nardin M D and Najafi K 2001 A self-oscillating detuning-insensitive class-E transmitter for implantable microsystems *IEEE Trans. Biomed. Eng.* **48** 397–400

Zierhofer C M and Hochmair E S 1990 High-efficiency coupling-insensitive transcutaneous power and data transmission via an inductive link *IEEE Trans. Biomed. Eng.* **37** 716–22